JACS
JOURNAL OF THE AMERICAN CHEMICAL SOCIETY
Article
Cite This: J. Am. Chem. Soc. XXXX, XXX, XXX−XXX
pubs.acs.org/JACS

Cytosolic Delivery of Proteins Using Amphiphilic Polymers with 2-Pyridinecarboxaldehyde Groups for Site-Selective Attachment

Rapeepat Sangsuwan,[†] Phum Tachachartvanich,[‡] and Matthew B. Francis*[,†,§]

[†]Department of Chemistry and [‡]Division of Environmental Health Sciences, School of Public Health, University of California, Berkeley, California 94720, United States

[§]Materials Sciences Division, Lawrence Berkeley National Laboratories, Berkeley, California 94720, United States

Supporting Information

ABSTRACT: Protein-based drugs are a promising class of therapeutics, but poor membrane permeability typically limits their application to extracellular receptors. Delivery strategies that can transport functional proteins to reach intracellular targets are needed, but with many current approaches, biomolecules become entrapped in the endosomes. This greatly reduces the effective concentrations of therapeutic agents at the target sites. Herein, we report a bioconjugation-based approach for intracellular protein delivery by site-selectively attaching amphiphilic polymers to the N-terminal positions of proteins using 2-pyridinecarboxaldehyde groups. The reaction is simple and features mild, aqueous conditions with no required genetic engineering of the proteins. Imaging studies demonstrate that the polymer−protein conjugates are successfully delivered into the cytosol of various cancer cell lines, likely through a membrane fusion mechanism. When conjugated to the delivery polymers, the activity of modified RNase A was retained and notably promoted cytotoxicity in cancer cells upon delivery to the cytosol. This work therefore provides a promising platform for protein-based material delivery for therapeutic applications.

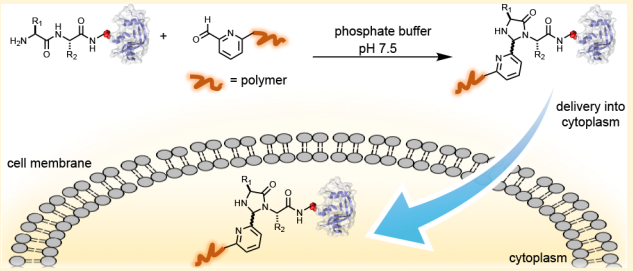

INTRODUCTION

Protein-based drugs are gaining significant interest due to their potential to engage macromolecular targets that are difficult to address using small molecules.[1−3] Since insulin was approved as the first recombinant protein therapeutic,[4] multiple engineered proteins have been developed for the treatment of diseases including hepatitis,[5] hemophilia,[6] and cancers.[7−10] Generally, proteins are membrane impermeable due to their large size,[11] which restricts their therapeutic use to extracellular targets. Proteins that are taken up intracellularly most often enter through the endocytosis pathway, meaning that after internalization the proteins are likely to be trapped in vesicles fated for lysosomal degradation.[12] Only a small number of therapeutic agents can escape from the endosomes to access the cytosol, and in most cases this severely reduces the biological activity that can be achieved for intracellular targets.[12] The development of efficient methods that deliver greater amounts of therapeutics to intracellular targets is thus critically important for the advancement of new biomolecule-based therapies.

A number of protein delivery technologies have emerged to address this limitation, such as cationic oligomers,[13] microgels,[14] nanoparticles,[15−17] and the direct incorporation of peptide transduction domains.[18,19] In the context of polymers, several approaches have been explored for assisted cytosolic delivery.[20,21] As one particularly promising lead, negatively charged and pH-responsive polyanion-based amphiphiles have previously been developed for delivery applications through endosomal escape mechanisms.[20,22−25] In a recent example, an amphiphilic polymer was used to coat quantum dots, which were transferred into the living cells.[26−32] This polymer has a water-soluble hydrophilic backbone partly substituted with hydrophobic alkyl chains that can embed into cell membranes.[26−32] Moreover, the polymaleic anhydride backbone used in this study is commercially available and provides a convenient route for incorporating additional synthetic groups into the polymer. On the basis of this precedent, we became interested in endowing these polymers with synthetic groups capable of site-specific bioconjugation, thus expanding their use to include a wide range of proteins of interest.

Existing bioconjugation reactions have contributed to the synthesis of many protein−polymer materials, though these methods often rely on nonspecific conjugations that can interfere with active sites or modify critical amino acid residues, resulting in an alteration of protein function. Ideally, one desires a well-defined protein bioconjugation reaction that occurs in water under mild pH and temperature conditions while also providing a high degree of selectivity to maintain biological efficacy. The reaction between the N-termini of proteins and 2-pyridinecarboxaldehyde (2PCA) has been reported by our laboratory as a one-step, site-specific method for protein modification, Figure 1.[33]

Received: October 15, 2018
Published: January 21, 2019

DOI: 10.1021/jacs.8b10947
J. Am. Chem. Soc. XXXX, XXX, XXX−XXX

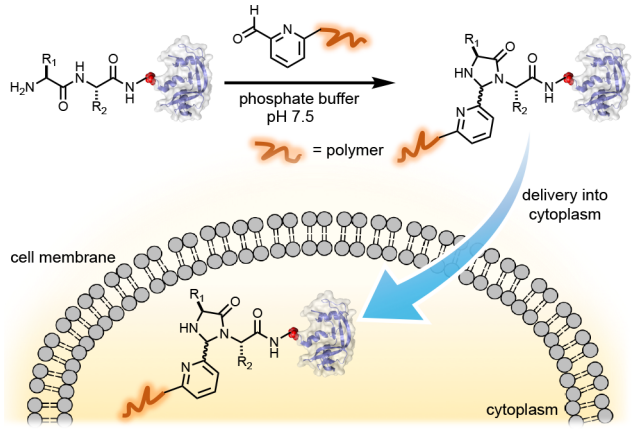

Figure 1. Schematic illustration of protein–polymer conjugate preparation using 2-pyridinecarboxaldehyde for N-terminal modification.

This reaction features mild conditions, is applicable to a broad set of proteins, and has a high tolerance toward a wide range of molecular weights, three-dimensional structures, and N-terminal amino acid residues. The only known incompatibilities for this chemistry are proteins with proline residues in the second position (which cannot undergo the cyclization reaction), proteins that are acylated or otherwise blocked at the N-terminus, and proteins that have N-termini that are not solution exposed. Otherwise, we have found that this conjugation chemistry is compatible with most expressed proteins with minimal if any genetic manipulation. Importantly, the N-terminal chemoselectivity of the reaction has been confirmed using protein digestion and MS/MS analyses.[33] This reaction has been successfully used to conjugate extracellular matrix (ECM) proteins to 2PCA-functionalized polyacrylamide hydrogels for cell adhesion, with the properties of the modified ECM proteins still being maintained after modification.[34]

Herein, we apply this N-terminal 2PCA modification reaction to prepare protein–polymer conjugates for cytosolic delivery (Figure 1). In initial studies, we attached green fluorescein protein (GFP) to polymers with different molar ratios of 2PCA groups and investigated the intracellular delivery of the conjugates into multiple types of cancer cells. The optimized construct showed substantial levels of delivery of the protein to the cytoplasm. Mechanistic studies further suggested that the conjugate likely avoids endosomal entrapment, instead entering the cell through a direct membrane interaction pathway. We used this polymer system to deliver ribonuclease A (RNase A), which is a protein that promotes cell death through cytosolic RNA degradation. We found that RNase A–polymer conjugates significantly decreased the viability of cancer cells upon delivery, suggesting that this strategy could likely be used in a number of future therapeutic applications.

RESULTS AND DISCUSSION

Polymer–Protein Conjugate Design and Polymer Synthesis. The polymer synthesis was modified from previous methods (Figure 2).[26−32] The maleic anhydride ring opening was carried out in the presence of reactive amines (dodecylamine and piperazinyl 2PCA, **A**) and trimethylamine. Following this, the remaining anhydride groups were hydrolyzed using aqueous NaOH. The reaction mixtures were

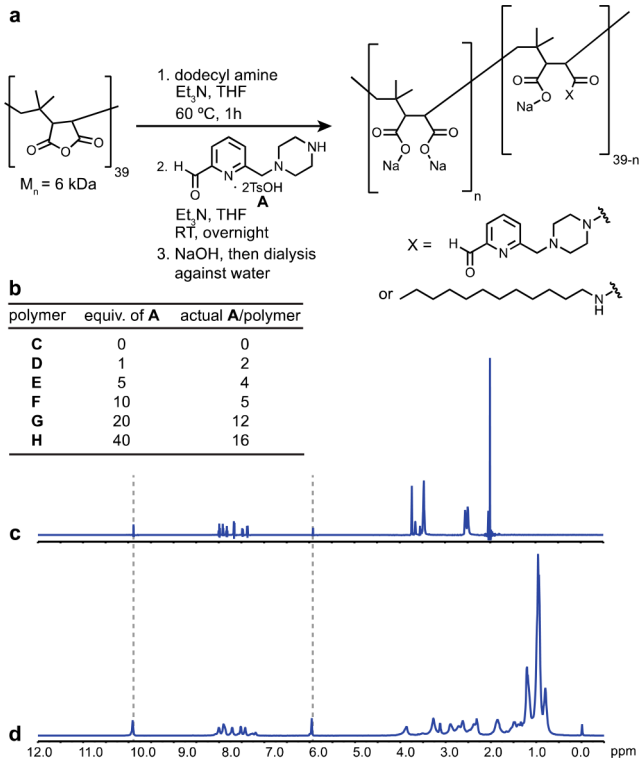

Figure 2. Synthesis and characterization of 2PCA-containing polymers. (a) Ring opening of poly(maleic anhydride) was performed using dodecylamine (6 equiv) followed by 2PCA-piperazine reagent **A** in the presence of triethylamine. (b) For the second amine addition, the amount of **A** was added at 0, 1, 5, 10, 20, and 40 equiv relative to the individual polymer strands. Using elemental analysis, the resulting levels of **A** incorporation were calculated. ^{1}H NMR spectra are shown for (c) the small-molecule 2PCA **B** and (d) polymer **H** in D_2O. Peaks corresponding to the aldehydes and their corresponding hydrates are indicated with dotted lines. For clarity, the water signal has been suppressed.

subsequently dialyzed against water and lyophilized. The polymer products were found to be completely water soluble. We hypothesized that different amounts of attached 2PCA would give different reactivities for the protein bioconjugation reaction, and this could influence the polymer–protein conjugate internalization. We therefore varied the ratio of **A** from 0 to 40 equiv with respect to the polymer strand to form polymers **C**–**H**, as indicated in Figure 2b.

NMR analysis of polymers **D**–**H** displayed characteristic aldehyde peaks, which aligned well with those of a 2PCA derivative **B**, Figure 2c and 2d and Supporting Information Figure S1. The peak at 6 ppm indicated the corresponding aldehyde hydrate, which is always observed for these compounds in aqueous samples. The NMR peak intensities (compared to the aliphatic protons) at 10 ppm increased from polymer **C** to **H**, suggesting that a higher amount of 2PCA moiety was incorporated into the polymer backbone (Supporting Information Figure S1). Elemental analysis was used to determine the percentage of C, H, and N atoms, and this information was used to estimate the numbers of 2PCA groups and alkyl chains (Figure 2b and Supporting Information Tables S1 and S2). The results indicated that increasing the amount of 2PCA influenced the magnitude of monomer modification, as expected. Small differences in the numbers of modified monomers were observed among **D**–**H**,

DOI: 10.1021/jacs.8b10947
J. Am. Chem. Soc. XXXX, XXX, XXX–XXX

which can be explained by the small molar ratios of **A** and the monomers compared to the polymers. For use in characterization and control experiments, a fluoresceinamine-substituted polymer and a 2PCA-5k polyethylene glycol (PEG) polymer[33] (**I**) were also synthesized (see Supporting Information for details).

2PCA Conjugation to GFP. The 2PCA reaction generates an imidazolidinone product through the nucleophilic attack on the initially formed N-terminal imine by the neighboring amide nitrogen on the protein backbone.[33] The chemoselectivity and reactivity of the 2PCA reaction was confirmed using 2PCA small molecule **B**, which readily coupled to GFP as seen in Figure 3a and 3b. GFP was chosen as the model protein because it also provided a fluorescent marker that would allow us to track intracellular protein localization. To verify whether the attachment occurred through the 2PCA reaction mechanism, hydroxylamine (NH_2OH) was reacted with an aldehyde group of 2PCA, which resulted in oxime formation. As expected, no N-terminal reactivity was observed in the presence of NH_2OH, as determined by ESI-TOF MS (Figure 3b).

We next optimized the conditions for protein–polymer conjugation according to previous work.[33] In general, the protein concentration did not significantly affect the reaction, and when the total 2PCA concentration was in the millimolar range, the reaction proceeded smoothly.[33] To confirm reactivity in the polymer context, GFP was mixed with the polymers (**C**–**H** or 2PCA-5k PEG **I**) for 18 h at 37 °C, and the products were analyzed by SDS-PAGE. The selectivity of the 2PCA groups was confirmed (Figure 3c and 3d) using polymer **C** (no 2PCA) and 2PCA-5k PEG **I** as negative and positive controls, respectively. As expected, polymer **C** did not conjugate to GFP, as no modified protein band was observed by SDS-PAGE, and polymer **I** afforded a single new high-molecular-weight band by SDS-PAGE, representing PEGylated GFP protein. Coincubation with NH_2OH did not show any 2PCA reactivity, which was consistent with the selectivity test performed with 2PCA mimic **B** (Figure 3b). Polymers **D**–**H** afforded a smeared band of modified proteins on SDS-PAGE due to the polydisperse nature of the polymers. Consistent with the findings for the PEG-2PCA reagent, no higher molecular weight bands were observed in the presence of NH_2OH. While it was difficult to quantify the intensities of the polymer–protein conjugates on the gel directly, densitometry measurements could be used to estimate the amount of free protein remaining after the conjugation reaction. Using this method it was determined that the coupling was ~68% complete in the case of polymer **H**.

Because the conjugation reaction involved a stoichiometric excess of polymer strands, the GFP–polymer conjugates were next purified to remove excess free polymer via Ni-NTA affinity chromatography. To prevent the capture of additional proteins in cell culture media, the remaining 2PCA aldehyde groups were inactivated with hydroxylamine before being carried forward to the intracellular delivery studies. Due to the large excess of 2PCA groups in the conjugation step, it was assumed that the number of polymer strands with more than one attached protein was negligible.

Intracellular Uptake of Protein–Polymer Conjugates and Uptake Mechanism Studies. The internalization of the GFP–polymer conjugates was investigated using the HeLa cell line as an initial model. Following 2 h of exposure at 10 μM, confocal microscopy analysis indicated that the GFP molecules

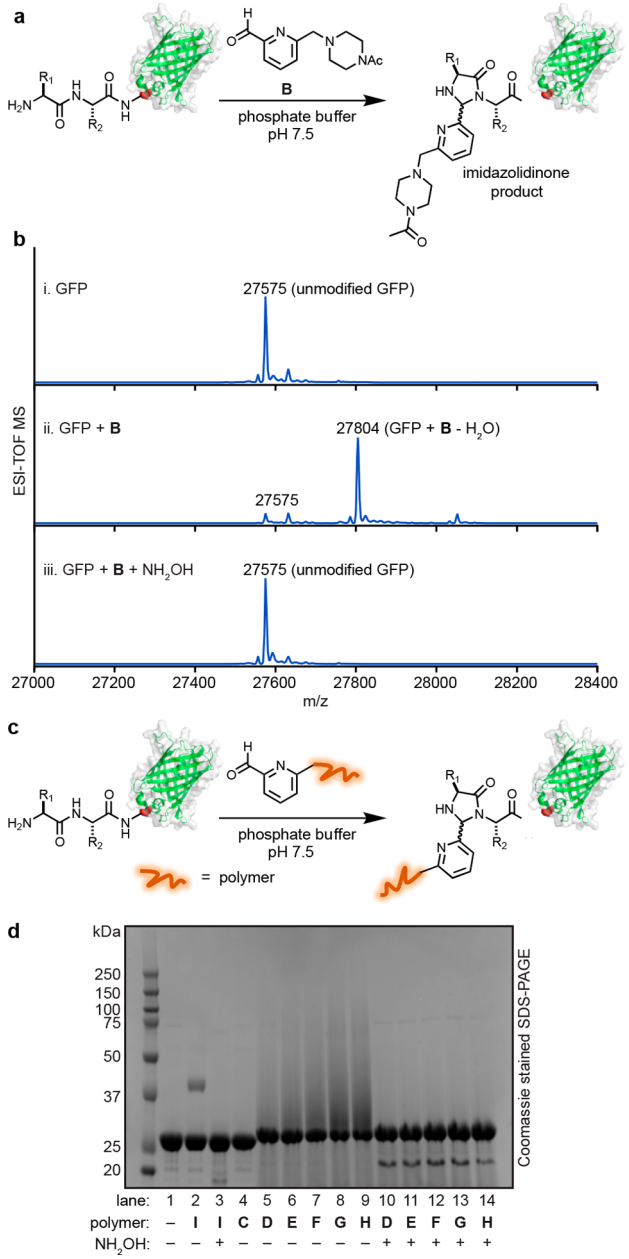

Figure 3. Coupling protein cargo to 2PCA-substituted polymers. (a) 2PCA reacts with N-terminal residues to form imidazolidinones. (b) ESI-TOF MS analyses are shown for GFP before and after the reaction with 2PCA reagent **B** or for **B** in the presence of NH_2OH as a coupling inhibitor. Reactions were run in 10 mM **B** and 10 μM protein, with or without 20 mM NH_2OH in 50 mM phosphate buffer, pH 7.5 at 37 °C for 18 h. (c) Coupling reactions were run with 20 mg/mL of polymer samples and 100 μM GFP with or without 200 mM NH_2OH in 50 mM phosphate buffer, pH 7.5 for 18 h at 37 °C. (d) Following SDS-PAGE, samples were visualized using Coomassie stain. **C** = polymer containing dodecylamine (no 2PCA), **D**–**H** = 2PCA-polymers (see Figure 2 for functionalization levels), **I** = 2PCA-5k PEG.

conjugated to polymer **H** were efficiently delivered into the cytosolic compartment, while GFP alone did not show detectable levels of delivery [Figure 4a (i and iii) and *z*-stacking images in Supporting Information Figure S2]. Increasing the equivalents of 2PCA on the polymers clearly increased the degree of conjugation and promoted greater

DOI: 10.1021/jacs.8b10947
J. Am. Chem. Soc. XXXX, XXX, XXX–XXX

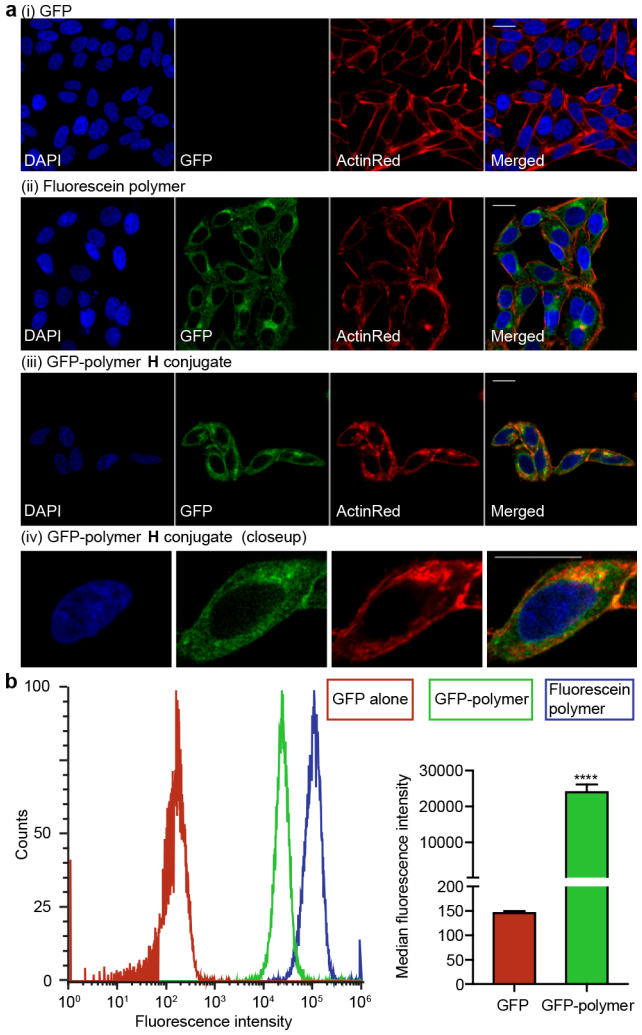

Figure 4. Uptake of GFP-labeled polymers into living cells. (a) Confocal microscopy images are shown for HeLa cells after exposure to GFP−polymer conjugates. Nuclear and cytoplasmic stains were performed on fixed cells using DAPI and ActinRed, respectively. Scale bars represent 20 μm. (b) HeLa cells were treated with GFP alone (10 μM), GFP conjugated to polymer **H** (10 μM), or fluorescein-labeled polymer (5 μM) for 2 h at 37 °C. Flow cytometry data are shown, along with the medians of the fluorescence intensity values. Error bars represent the standard errors resulting from three independent experiments. ****p < 0.0001 indicates a significant difference between GFP−polymer-treated cells and unmodified GFP-treated cells.

cellular uptake of the proteins, as observed by the increased fluorescence (Supporting Information Figure S3). However, there was little difference observed in internalization levels for the different polymers among **D**, **E**, and **F** or between **G** and **H**, which agreed well with the elemental analysis results that all polymers had a similar amount of 2PCA on the polymer backbone (Figure 2b). The delivery of the fluorescein-tagged polymer at 5 μM was confirmed as a positive control [Figure 4a (ii)]. Polymer **H** was used for further study as it showed the most efficient delivery levels.

We next investigated the effects of protein concentration on delivery efficiency of GFP−polymer **H** into HeLa cells. The uptake was observed to increase with increasing concentrations of the protein (Supporting Information Figure S4). Conjugate concentrations as low as 50 nM still led to detectable uptake. In all cases, diffuse cytoplasmic fluorescence was observed, suggesting that the entry mechanism was not affected by the concentration. In a separate series of experiments, confocal images were acquired at different time points for a 10 μM sample of GFP−polymer **H** (Supporting Information Figure S5). Binding of the cell membrane was observed after 10 min, and the conjugates entered the cytoplasm gradually over a period of 30−180 min. These results bear some similarity to those of Mout et al., who used gold nanoparticle coassembly techniques for the delivery of GFP into SKOV-3 cells,[35] although the entry of the GFP−polymer **H** occurs on a slower time scale than that observed in their studies.

Flow cytometry was also used to investigate the protein delivery, showing a >100-fold difference in cellular uptake between unmodified GFP and the GFP−polymer conjugate, Figure 4b. An additional toxicity study of both the conjugate and the free polymer was carried out to ensure that the concentrations used for the cell treatment did not interfere with cell viability (Supporting Information Figure S6). In addition to HeLa cells, the protein conjugate could be delivered into other cancer cell types (lung [A549], breast [MCF7], prostate [PC-3], and brain [U-87 MG]), demonstrating that the approach is likely to be applicable to many cell types (Supporting Information Figures S7−S10). Following delivery, some differences in subcellular localization could be observed for the GFP−polymer **H** conjugates across the cell lines that were studied; however, at least some diffuse cytoplasmic fluorescence was observed in each case.

Experiments were also run to study the uptake mechanisms for the conjugates (Figure 5). Inhibitors of clathrin-dependent endocytosis (chlorpromazine and wortmannin)[36−40] did not significantly attenuate cellular internalization of the GFP−polymer **H** conjugate. Other inhibitors of caveolae-dependent endocytosis and macropinocytosis uptake pathways also did not block the translocation of the GFP−polymer **H** conjugate (Supporting Information Figure S11). To confirm that the polymer did not compromise the integrity of the cell membranes to allow diffusive entry, cells were cotreated with free GFP and free polymer that was previously inactivated with hydroxylamine. No intracellular internalization of GFP was seen in these experiments.

The only additive that prevented the uptake of the conjugates was methyl-β-cyclodextrin (Figure 5(iv)), which is known to inhibit both endocytosis and membrane fusion mechanisms by removing cholesterol from plasma membranes.[41,42] Because none of the other small molecule inhibitors blocked uptake, we favor the interpretation that conjugate entry occurs through the fusion mechanism. For the HeLa cells that were examined in these experiments, there was also a lack of distinct puncta that would indicate the presence of endocytotic vesicles prior to rupture. Such species have been observed in other delivery studies that involve endosomal escape pathways and look quite different from the images reported herein.[43,44] Other cell lines did show increased numbers of localized fluorescence signals (Supporting Information Figures S7−S10), but they were always accompanied by broad cytoplasmic fluorescence. It can be difficult to distinguish between endocytotic disruption and membrane fusion membranes in general, and the pathways can be cell line dependent. Given those caveats, the data currently suggest that the vesicle fusion pathway is the more likely mechanism of entry for these polymer−protein conjugates. This would be highly preferable, as such a pathway would avoid the

DOI: 10.1021/jacs.8b10947
J. Am. Chem. Soc. XXXX, XXX, XXX−XXX

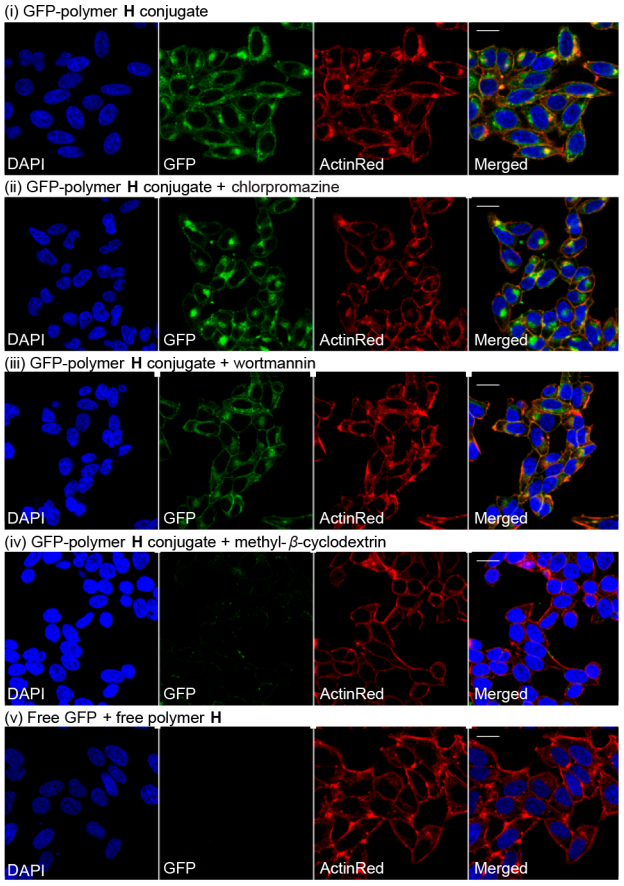

Figure 5. Probing the uptake mechanism of GFP–polymer conjugates in HeLa cells using confocal microscopy. HeLa cells were pretreated with corresponding inhibitors for 30 min prior to a 2 h cotreatment with GFP conjugated to polymer **H** and inhibitors (5.7 mM methyl-β-cyclodextrin, 10 μM chlorpromazine, or 0.35 μM wortmannin). As a control experiment, cells were coincubated with 10 μM free GFP and 10 μM polymer **H** (with no attached protein). Nuclear and cytoplasmic stains were performed on fixed cells using DAPI and ActinRed, respectively. Scale bars represent 20 μm.

acidification and proteolysis events that can inactivate proteins following uptake into vesicles.

It is important to note that the polymer remains attached to the protein after it is delivered into the cells, which would limit this approach for the delivery of transcription factors and other proteins that require nuclear localization for proper function. In current work we are designing versions of the polymers that will cleave upon cellular entry to prevent this limitation. Nonetheless, the approach is likely to be useful for the delivery of many proteins with cytosolic function in its current form.

Delivery of RNase A as a Cytotoxic Cargo Protein. The results of the GFP–polymer delivery studies indicated that this approach facilitates the internalization of proteins from the extracellular environment into the cytosolic compartment of cells. Next, a study was performed to elucidate the integrity and functionality of delivered modified proteins. RNase A catalyzes the degradation of RNA strands and promotes cancer cell death if it is internalized into the cytosol.[45−47] It therefore served as a model functional protein for testing cytosolic delivery. The selectivity of the 2PCA reaction was first assessed using ESI-TOF MS and SDS-PAGE (Supporting Information Figures S12 and S13). The data showed that 2PCA mimic **B** did conjugate to the N-terminus of RNase A. With NH_2OH quenching, there was no reactivity observed. SDS-PAGE analyses confirmed polymer attachment, with the level of conversion estimated at 73% based on densitometry quantification of the remaining free protein.

The enzymatic activities of RNase A and the RNase A–polymer conjugate were assessed as previously described.[48] The absorbance of a solution containing RNA oligos and RNase A or the RNase–polymer conjugate was monitored at 300 nm at 1 min intervals, and the decrease in absorption intensity as a result of the RNA degradation was observed (Figure 6). Both RNase A and the RNase-polymer conjugate showed similar enzymatic activity, which indicated that polymer conjugation did not affect the activity of protein.

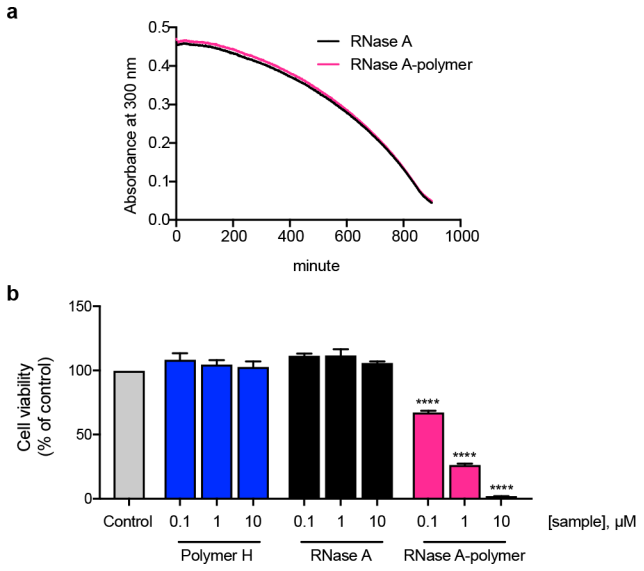

Figure 6. Delivery of RNase A to cells as a model cytotoxic cargo molecule. (a) Enzymatic activity of RNase A is unaffected by polymer attachment. Absorbance at 300 nm was recorded at 1 min intervals. (b) HeLa cells were incubated alone (control), with polymer **H**, or with the conjugate of RNase A to polymer **H** for 6 h at 37 °C. Viability was measured using an MTT assay and is reported as the percentage of surviving cells compared to the untreated control. Error bars represent the standard error of three independent experiments. ****$p < 0.0001$ indicates a significant difference between RNase A-polymer **H**-treated cells and unmodified RNase A-treated cells.

We next confirmed the integrity and functionality of the RNase–polymer conjugate in cell culture. HeLa cells were exposed to solutions of unconjugated polymer **H**, free RNase A, and the RNase A–polymer **H** conjugate at 37 °C. Cell viability was then determined using an MTT assay. After a 6 h treatment, the RNase A–polymer conjugate exhibited a notable cytotoxic effect, while the unconjugated polymer **H** and unmodified RNase A treatments did not significantly lower cell viability, Figure 6b. It is worth noting that the RNase A–polymer conjugate elicited significant cytotoxicity in a dose-dependent manner, indicating that the method successfully modified and delivered functional protein intracellularly.

CONCLUSIONS

In the present work, we demonstrate a polymer designed to facilitate protein-based drug delivery. The polymer has both hydrophobic and hydrophilic properties, 2PCA moieties for conjugation, and excellent water solubility. The 2PCA

DOI: 10.1021/jacs.8b10947
J. Am. Chem. Soc. XXXX, XXX, XXX−XXX

conjugation is simple and occurs specifically at the N-termini of proteins, which provides site-selective functionalization for many different biomolecules in a location that minimally affects structure and function. We also show that this strategy both delivers proteins into the cytosolic compartment and preserves their integrity and functionality, which are key for therapeutics. Current data suggest that the internalization pathway of the construct is likely to be mediated through a membrane fusion mechanism without membrane disruption, at least partially circumventing the protein degradation that occurs through endocytosis. Delivery success is not cell-type specific, making it possible to apply this polymer conjugation technology for a wide range of applications in different cell types. This work therefore provides a promising platform for protein-based material delivery for therapeutic applications.

EXPERIMENTAL SECTION

Synthesis of Dodecylamine-, 2-Pyridinecarbozaldehyde-, and Fluoresceinamine-Modified Poly(isobutylene-*alt*-maleic Anhydride) Derivatives. The synthesis was modified from the previously reported protocol.[26−32] A flame-dried 250 mL round-bottom flask was charged with 100 mg of poly(isobutylene-*alt*-maleic anhydride) (average molecular weight 6000 g/mol, 0.017 mmol) in 30 mL of dry THF. Dodecylamine (18 mg, 0.1 mmol, 6 equiv relative to the polymer strands) and dry triethylamine (28 μL, 0.2 mmol) were dissolved in 5 mL of dry THF and added dropwise. The solution was stirred 1 h at 60 °C. The temperature was reduced to room temperature and varying amounts of **A** (9.2, 46, 92, 183, and 366 mg: 0.017, 0.083, 0.17, 0.33, and 0.66 mmol, respectively, or 1, 5, 10, 20, and 40 equiv relative to the polymer strands, respectively) along with triethylamine (2 equiv relative to **A**). For the fluoresceinamine-labeled polymer, fluoresceinamine isomerically pure dye (5-isomer) (16.9 mg, 0.033 mmol) along with triethylamine (9 μL, 0.066 mmol) dissolved in THF (15 mL) were added dropwise. The solution was allowed to stir overnight at room temperature. The solvent and excess triethylamine were removed under reduced pressure, and the resulting residue was dissolved in aqueous 27.5 mM NaOH. The solution was dialyzed against several changes of deionized water over multiple days and lyophilized to yield 130−139 mg of the polymer products.

General Procedure for the Reaction of 2PCA B with Proteins. A 5 μL aliquot was taken from a 1 mM solution of protein (final concentration of 100 μM) and added to 40 μL of 50 mM phosphate buffer at pH 7.5 with or without 20 mM NH_2OH (which was only used in control experiments). To the resulting solution was added a 5 μL aliquot of a 100 mM solution of **B** in H_2O (final concentration of 10 mM). The reaction was briefly agitated to ensure proper mixing and incubated at 25 or 37 °C without further mixing. The reaction product was purified using a 0.5 mL Amicon Ultra-4 centrifugal filter unit with an appropriate molecular weight cut off (EMD Millipore). Modification was monitored by LC-MS.

General Procedure for the Reaction of 2-Pyridinecarboxaldehyde Polymers with Proteins. A 100 μL aliquot was taken from a 1 mM solution of protein (final concentration of 100 μM) and added to 400 μL of 50 mM phosphate buffer at pH 7.5. To the resulting solution was added a 500 μL of 40 mg/mL solution of polymer in the same buffer. The reaction was briefly agitated to ensure proper mixing and incubated at 25 or 37 °C without further agitation. The reaction mixtures containing sfGFP−polymer conjugates were purified by HisPur Ni-NTA spin columns (Thermo Fisher) according to the manufacturer's instructions. For RNase A−polymer conjugates, the reactions were purified using Pierce strong cation-exchange spin columns (Thermo Fisher) according to the manufacturer's instructions. The purified proteins were treated with 5 mM NH_2OH for 10 min at room temperature and then desalted against 10 mM phosphate buffer at pH 7.5 by using PD MidiTrap G-10 columns (GE Healthcare). Protein concentration was determined using a BCA assay (Thermo Fisher).

Cell Culture. All cell lines (HeLa, A549, PC-3, MCF7, and U-87 MG) were cultured in DMEM (Gibco) supplemented with 2 mM L-glutamine (Gibco), 100 IU/mL penicillin, 100 μg/mL streptomycin (Gibco), and 10% (v/v) fetal bovine serum (FBS, Gibco). For the PC-3 cell line, the media were additionally supplemented with MEM nonessential amino acids solution (1×, Gibco). For MCF7 and U-87 MG cell lines, the media were additionally supplemented with 1 mM sodium pyruvate and MEM nonessential amino acids solution (1×, Gibco). All cell lines were maintained at 37 °C in a humidified atmosphere containing 95% air and 5% CO_2.

Flow Cytometry Analysis. HeLa cells were treated with sfGFP (10 μM), sfGFP−polymer conjugate (10 μM), or fluorescein-coupled polymer (5 μM) for 2 h at 37 °C. The treated cells were then washed trice with Dulbecco's phosphate-buffered saline (DPBS), followed by cell dissociation buffer (Gibco) at 37 °C for 5 min. The released cells were then pelleted and resuspended in DPBS to a density of 1×10^6 cells/mL and analyzed by flow cytometry (Attune NxT flow cytometer, Thermo Fisher). For each sample, 20 000 cells were counted. Gating was performed by applying the autogating function on the major population of cells in the FSC × SSC (forward versus side scatter plots) of untreated samples; the treated samples were subject to the same gating as the untreated populations.

Confocal Microscopy. Cells were washed with DPBS and trypsinized; then the trypsin was quenched with complete growth media. The resulting cells were resuspended in growth media at a concentration of 50 000 cells/mL, and 0.5 mL of the cell suspension was added to each section of an 8-well chambered coverglass (LabTek). Cells were allowed to grow at 37 °C with 5% CO_2 for 72 h. Media were aspirated, and the cells were washed twice with 0.5 mL of complete media. Samples were then added to each well at a final concentration of 1−10 μM 2PCA protein−polymer conjugate, 0.5−10 μM fluorescein-coupled polymer, or 1−10 μM unmodified protein in a total of 200 μL of media. The dishes were incubated at 37 °C with 5% CO_2 for 2 h, and then the cells were washed twice with 0.5 mL of DPBS. The cells were fixed with DAPI (1 μg/mL, Thermo Fisher) in 4% formaldehyde in DPBS for 10 min at room temperature. The cells were washed trice with DPBS (5 min incubation) and incubated with 0.1% triton X in DPBS at room temperature for 15 min, followed by three washes with DPBS. The cells were stained with an ActinRed ready probe (Thermo Fisher) according to the manufacturer's instructions. Images were acquired on a Zeiss LSM710 laser-scanning microscope, usage courtesy of Professor Christopher Chang (UC Berkeley).

Internalization Mechanism Study. Cells were grown and seeded in an 8-well chambered coverglass (LabTek) setup as described above. Cells were pretreated with inhibitors (5.7 mM methyl-β-cyclodextrin, 10 μM chlorpromazine, 0.35 μM wortmannin, 50 μM dynasore, or 30 μM amiloride) at 37 °C for 30 min. Following this was a 2 h treatment (37 °C) with 10 μM protein with or without 10 μM polymers, as reported previously.[36−39,41] Nuclear and cytoplasmic staining were performed using DAPI and ActinRed, as described above.

RNase A Activity Assay. The protocol used in these experiments was reported previously.[48] A 50 μL aliquot was taken from a 1 mg/mL solution of RNase A or its polymer conjugate and added to 50 μL of RNA from a 4 mg/mL 100 mM sodium acetate, pH 5.0 at 25 °C in a 96-well plate (Thermo Fisher). The absorbance at 300 nm was monitored over time by an Infinite 200 Pro plate reader (Tecan, Switzerland).

Cell Viability Assays. The protocol was modified from a previously described procedure.[49,50] Cells were trypsinized and diluted to a density of 50 000 cells/mL. An aliquot of 200 μL of cell stock was placed in a well of a 96-well plate (Corning) to reach a density of 10 000 cells/well. The plate was incubated at 37 °C in a 5% CO_2 atmosphere for 18 h. Media were removed from the plate, and 100 μL portions of the appropriate sample stocks in media were added. The cells were incubated at 37 °C in a 5% CO_2 atmosphere for a determined time (2−18 h). The medium containing the sample was removed from the well, and 100 μL of 3-(4,5-dimethylthiazol-2-yl)-2,5-diphenyl-tetrazolium bromide (MTT) in serum free media (0.5

DOI: 10.1021/jacs.8b10947
J. Am. Chem. Soc. XXXX, XXX, XXX−XXX

mg/mL, Amresco) was added to each well. The samples were incubated for 4 h. An Infinite 200 Pro plate reader (Tecan) was used to measure the absorbance at 570 nm.

■ ASSOCIATED CONTENT

Supporting Information

The Supporting Information is available free of charge on the ACS Publications website at DOI: 10.1021/jacs.8b10947.

Experimental details and supporting figures and tables (PDF)

■ AUTHOR INFORMATION

Corresponding Author

*E-mail: mbfrancis@berkeley.edu

ORCID

Rapeepat Sangsuwan: 0000-0003-0836-4514

Phum Tachachartvanich: 0000-0002-9783-6482

Matthew B. Francis: 0000-0003-2837-2538

Notes

The authors declare no competing financial interest.

■ ACKNOWLEDGMENTS

This work was generously supported by the NSF (CHE 1808189). We thank Dr. Alan Marmelstein for comments and suggestions on the manuscript as well as Emmy Tian for assisting in the synthesis of polymers. We also acknowledge Prof. Christopher Chang and Dr. Lakshmipriya Krishnamoorthy (UC Berkeley) for confocal microscopy usage.

■ REFERENCES

(1) Leader, B.; Baca, Q. J.; Golan, D. E. Protein therapeutics: a summary and pharmacological classification. *Nat. Rev. Drug Discovery* **2008**, *7* (1), 21−39.

(2) Bruno, B. J.; Miller, G. D.; Lim, C. S. Basics and recent advances in peptide and protein drug delivery. *Ther. Delivery* **2013**, *4* (11), 1443−1467.

(3) Craik, D. J.; Fairlie, D. P.; Liras, S.; Price, D. The Future of Peptide-based Drugs. *Chem. Biol. Drug Des.* **2013**, *81* (1), 136−147.

(4) Golan, D. E.; Tashjian, A. H.; Armstrong, E. J. *Principles of pharmacology: the pathophysiologic basis of drug therapy*; Lippincott Williams & Wilkins, 2011.

(5) Lindsay, K. L. Therapy of hepatitis C: overview. *Hepatology* **1997**, *26* (S3), 71S−77S.

(6) Roth, D. A.; Kessler, C. M.; Pasi, K. J.; Rup, B.; Courter, S. G.; Tubridy, K. L. Human recombinant factor IX: safety and efficacy studies in hemophilia B patients previously treated with plasma-derived factor IX concentrates. *Blood* **2001**, *98* (13), 3600−3606.

(7) *Information on Cetuximab (marketed as Erbitux)*; U.S. Food and Drug Administration: Silver Spring, MD, 2004 (accessed Aug 25, 2018).

(8) Goldman, S. C.; Holcenberg, J. S.; Finklestein, J. Z.; Hutchinson, R.; Kreissman, S.; Johnson, F. L.; Tou, C.; Harvey, E.; Morris, E.; Cairo, M. S. A randomized comparison between rasburicase and allopurinol in children with lymphoma or leukemia at high risk for tumor lysis: Presented in part at the American Society of Hematology Conference in Miami Beach, FL, December 1998. *Blood* **2001**, *97* (10), 2998−3003.

(9) Hurwitz, H.; Fehrenbacher, L.; Novotny, W.; Cartwright, T.; Hainsworth, J.; Heim, W.; Berlin, J.; Baron, A.; Griffing, S.; Holmgren, E. Bevacizumab plus irinotecan, fluorouracil, and leucovorin for metastatic colorectal cancer. *N. Engl. J. Med.* **2004**, *350* (23), 2335−2342.

(10) Vogel, C. L.; Cobleigh, M. A.; Tripathy, D.; Gutheil, J. C.; Harris, L. N.; Fehrenbacher, L.; Slamon, D. J.; Murphy, M.; Novotny, W. F.; Burchmore, M. Efficacy and safety of trastuzumab as a single agent in first-line treatment of HER2-overexpressing metastatic breast cancer. *J. Clin. Oncol.* **2002**, *20* (3), 719−726.

(11) Yang, N. J.; Hinner, M. J. Getting across the cell membrane: an overview for small molecules, peptides, and proteins. *Site-Specific Protein Labeling*; Springer, 2015; pp 29−53.

(12) Kou, L.; Sun, J.; Zhai, Y.; He, Z. The endocytosis and intracellular fate of nanomedicines: Implication for rational design. *Asian J. Pharm. Sci.* **2013**, *8* (1), 1−10.

(13) Liu, X.; Zhang, P.; He, D.; Rödl, W.; Preiß, T.; Rädler, J. O.; Wagner, E.; Lächelt, U. pH-Reversible Cationic RNase A Conjugates for Enhanced Cellular Delivery and Tumor Cell Killing. *Biomacromolecules* **2016**, *17* (1), 173−182.

(14) Murthy, N.; Thng, Y. X.; Schuck, S.; Xu, M. C.; Fréchet, J. M. A novel strategy for encapsulation and release of proteins: hydrogels and microgels with acid-labile acetal cross-linkers. *J. Am. Chem. Soc.* **2002**, *124* (42), 12398−12399.

(15) Maier, K.; Martin, I.; Wagner, E. Sequence defined disulfide-linked shuttle for strongly enhanced intracellular protein delivery. *Mol. Pharmaceutics* **2012**, *9* (12), 3560−3568.

(16) Mout, R.; Ray, M.; Tay, T.; Sasaki, K.; Yesilbag Tonga, G.; Rotello, V. M. General Strategy for Direct Cytosolic Protein Delivery via Protein-Nanoparticle Co-engineering. *ACS Nano* **2017**, *11* (6), 6416−6421.

(17) Mout, R.; Yesilbag Tonga, G.; Wang, L.-S. S.; Ray, M.; Roy, T.; Rotello, V. M. Programmed Self-Assembly of Hierarchical Nanostructures through Protein-Nanoparticle Coengineering. *ACS Nano* **2017**, *11* (4), 3456−3462.

(18) Nischan, N.; Herce, H. D.; Natale, F.; Bohlke, N.; Budisa, N.; Cardoso, M. C.; Hackenberger, C. P. Covalent attachment of cyclic TAT peptides to GFP results in protein delivery into live cells with immediate bioavailability. *Angew. Chem., Int. Ed.* **2015**, *54* (6), 1950−1953.

(19) Akishiba, M.; Takeuchi, T.; Kawaguchi, Y.; Sakamoto, K.; Yu, H.-H.; Nakase, I.; Takatani-Nakase, T.; Madani, F.; Gräslund, A.; Futaki, S. Cytosolic antibody delivery by lipid-sensitive endosomolytic peptide. *Nat. Chem.* **2017**, *9* (8), 751.

(20) Guo, S.; Huang, L. Nanoparticles escaping RES and endosome: challenges for siRNA delivery for cancer therapy. *J. Nanomater.* **2011**, *2011*, 742895.

(21) Wu, Y.; Smith, A. E.; Reineke, T. M. Lipophilic Polycation Vehicles Display High Plasmid DNA Delivery to Multiple Cell Types. *Bioconjugate Chem.* **2017**, *28* (8), 2035−2040.

(22) Convertine, A. J.; Diab, C.; Prieve, M.; Paschal, A.; Hoffman, A.; Johnson, P.; Stayton, P. S. pH-responsive polymeric micelle carriers for siRNA drugs. *Biomacromolecules* **2010**, *11* (11), 2904−2911.

(23) Kyriakides, T. R.; Cheung, C. Y.; Murthy, N.; Bornstein, P.; Stayton, P. S.; Hoffman, A. S. pH-sensitive polymers that enhance intracellular drug delivery in vivo. *J. Controlled Release* **2002**, *78* (1−3), 295−303.

(24) Jones, R. A.; Cheung, C. Y.; Black, F. E.; Zia, J. K.; Stayton, P. S.; Hoffman, A. S.; Wilson, M. R. Poly (2-alkylacrylic acid) polymers deliver molecules to the cytosol by pH-sensitive disruption of endosomal vesicles. *Biochem. J.* **2003**, *372* (1), 65−75.

(25) Cheung, C. Y.; Murthy, N.; Stayton, P. S.; Hoffman, A. S. A pH-sensitive polymer that enhances cationic lipid-mediated gene transfer. *Bioconjugate Chem.* **2001**, *12* (6), 906−910.

(26) Jańczewski, D.; Tomczak, N.; Han, M.-Y.; Vancso, G. J. Synthesis of functionalized amphiphilic polymers for coating quantum dots. *Nat. Protoc.* **2011**, *6* (10), 1546.

(27) Lin, C. A. J.; Sperling, R. A.; Li, J. K.; Yang, T. Y.; Li, P. Y.; Zanella, M.; Chang, W. H.; Parak, W. J. Design of an amphiphilic polymer for nanoparticle coating and functionalization. *Small* **2008**, *4* (3), 334−341.

(28) Jańczewski, D.; Tomczak, N.; Khin, Y. W.; Han, M.-Y.; Vancso, G. J. Designer multi-functional comb-polymers for surface engineering of quantum dots on the nanoscale. *Eur. Polym. J.* **2009**, *45* (1), 3−9.

(29) Jańczewski, D.; Tomczak, N.; Han, M.-Y.; Vancso, G. J. Introduction of quantum dots into PNIPAM microspheres by

DOI: 10.1021/jacs.8b10947
J. Am. Chem. Soc. XXXX, XXX, XXX−XXX

precipitation polymerization above LCST. *Eur. Polym. J.* **2009**, *45* (7), 1912−1917.
(30) Jańczewski, D.; Tomczak, N.; Song, J.; Long, H.; Han, M.-Y.; Vancso, G. J. Fabrication and responsive behaviour of Quantum Dot/PNIPAM micropatterns obtained by template copolymerization in water. *J. Mater. Chem.* **2011**, *21* (18), 6487−6490.
(31) Tomczak, N.; Jaczewski, D.; Tagit, O.; Han, M. Y.; Vancso, G. J. Surface engineering of quantum dots with designer ligands. *Surface Design: Applications in Bioscience and Nanotechnology*; Wiley-VCH Verlag GmbH & Co. KGaA: Weinheim, Germany, 2009; pp 341−361.
(32) Tagit, O.; Jańczewski, D.; Tomczak, N.; Han, M. Y.; Herek, J. L.; Vancso, G. J. Nanostructured thermoresponsive quantum dot/PNIPAM assemblies. *Eur. Polym. J.* **2010**, *46* (7), 1397−1403.
(33) MacDonald, J. I.; Munch, H. K.; Moore, T.; Francis, M. B. One-step site-specific modification of native proteins with 2-pyridinecarboxyaldehydes. *Nat. Chem. Biol.* **2015**, *11* (5), 326.
(34) Lee, J. P.; Kassianidou, E.; MacDonald, J. I.; Francis, M. B.; Kumar, S. N-terminal specific conjugation of extracellular matrix proteins to 2-pyridinecarboxaldehyde functionalized polyacrylamide hydrogels. *Biomaterials* **2016**, *102*, 268−276.
(35) Mout, R.; Ray, M.; Tay, T.; Sasaki, K.; Yesilbag Tonga, G.; Rotello, V. M. General Strategy for Direct Cytosolic Protein Delivery via Protein−Nanoparticle Co-engineering. *ACS Nano* **2017**, *11* (6), 6416−6421.
(36) Saha, K.; Kim, S. T.; Yan, B.; Miranda, O. R.; Alfonso, F. S.; Shlosman, D.; Rotello, V. M. Surface functionality of nanoparticles determines cellular uptake mechanisms in mammalian cells. *Small* **2013**, *9* (2), 300−305.
(37) Gratton, S. E.; Ropp, P. A.; Pohlhaus, P. D.; Luft, J. C.; Madden, V. J.; Napier, M. E.; DeSimone, J. M. The effect of particle design on cellular internalization pathways. *Proc. Natl. Acad. Sci. U. S. A.* **2008**, *105* (33), 11613−11618.
(38) Zhang, L. W.; Monteiro-Riviere, N. A. Mechanisms of quantum dot nanoparticle cellular uptake. *Toxicol. Sci.* **2009**, *110* (1), 138−155.
(39) Plummer, E. M.; Manchester, M. Endocytic Uptake Pathways Utilized by CPMV Nanoparticles. *Mol. Pharmaceutics* **2013**, *10* (1), 26−32.
(40) Bandmann, V.; Müller, J. D.; Köhler, T.; Homann, U. Uptake of fluorescent nano beads into BY2-cells involves clathrin-dependent and clathrin-independent endocytosis. *FEBS Lett.* **2012**, *586* (20), 3626−3632.
(41) Yang, S.-T.; Kreutzberger, A. J.; Lee, J.; Kiessling, V.; Tamm, L. K. The role of cholesterol in membrane fusion. *Chem. Phys. Lipids* **2016**, *199*, 136−143.
(42) Juliano, R. L. The delivery of therapeutic oligonucleotides. *Nucleic Acids Res.* **2016**, *44* (14), 6518−6548.
(43) Zhang, P.; He, D.; Klein, P. M.; Liu, X.; Röder, R.; Döblinger, M.; Wagner, E. Enhanced Intracellular Protein Transduction by Sequence Defined Tetra-Oleoyl Oligoaminoamides Targeted for Cancer Therapy. *Adv. Funct. Mater.* **2015**, *25* (42), 6627−6636.
(44) Wang, M.; Zuris, J. A.; Meng, F.; Rees, H.; Sun, S.; Deng, P.; Han, Y.; Gao, X.; Pouli, D.; Wu, Q. Efficient delivery of genome-editing proteins using bioreducible lipid nanoparticles. *Proc. Natl. Acad. Sci. U. S. A.* **2016**, *113* (11), 2868−2873.
(45) Leland, P. A.; Raines, R. T. Cancer chemotherapy−ribonucleases to the rescue. *Chem. Biol.* **2001**, *8* (5), 405−413.
(46) Raines, R. T. Ribonuclease a. *Chem. Rev.* **1998**, *98* (3), 1045−1066.
(47) Shlyakhovenko, V. A. Ribonucleases in tumor growth. *Exp. Oncol.* **2009**, *31*, 127−133.
(48) Kunitz, M. A spectrophotometric method for the measurement of ribonuclease activity. *J. Biol. Chem.* **1946**, *164*, 563−568.
(49) Suriyo, T.; Tachachartvanich, P.; Visitnonthachai, D.; Watcharasit, P.; Satayavivad, J. Chlorpyrifos promotes colorectal adenocarcinoma H508 cell growth through the activation of EGFR/ERK1/2 signaling pathway but not cholinergic pathway. *Toxicology* **2015**, *338*, 117−129.
(50) Tachachartvanich, P.; Sangsuwan, R.; Ruiz, H. S.; Sanchez, S. S.; Durkin, K. A.; Zhang, L.; Smith, M. T. Assessment of the Endocrine-Disrupting Effects of Trichloroethylene and Its Metabolites Using in Vitro and in Silico Approaches. *Environ. Sci. Technol.* **2018**, *52* (3), 1542−1550.

DOI: 10.1021/jacs.8b10947
J. Am. Chem. Soc. XXXX, XXX, XXX−XXX